Access Point Selection Scheme for LiFi Cellular Networks using Angle Diversity Receivers

Citation for published version:
Zeng, Z, Dehghani Soltani, M, Wu, X & Haas, H 2019, Access Point Selection Scheme for LiFi Cellular Networks using Angle Diversity Receivers. in *IEEE Wireless Communications and Networking Conference (WCNC).* IEEE Wireless Communications and Networking Conference (WCNC), IEEE, IEEE Wireless Communications and Networking Conference, Marrakech, Morocco, 15/04/19. https://doi.org/10.1109/WCNC.2019.8885720

Digital Object Identifier (DOI):
10.1109/WCNC.2019.8885720

Link:
Link to publication record in Edinburgh Research Explorer

Document Version:
Peer reviewed version

Published In:
IEEE Wireless Communications and Networking Conference (WCNC)

Access Point Selection Scheme for LiFi Cellular Networks using Angle Diversity Receivers

Zhihong Zeng, Mohammad Dehghani Soltani, Xiping Wu and Harald Haas
LiFi R&D Centre, Institute for Digital Communications, School of Engineering, The University of Edinburgh
E-mail: {zhihong.zeng, m.dehghani, xiping.wu, h.haas}@ed.ac.uk

***Abstract*—Light Fidelity (LiFi) is an emerging technology for future high-speed indoor wireless communications. Co-channel interference (CCI) caused by the dense deployment of LiFi access points (APs) can be effectively mitigated by using angle diversity receivers (ADRs). ADRs require signal combining where the combining weights depend on the selection of serving APs. In this paper, the AP selection (APS) strategy considering handover is studied. A novel APS scheme based on evolutionary game theory (EGT) is proposed for the LiFi network using ADRs. The performance of the proposed scheme is comprehensively analysed and compared with the APS scheme based on signal strength strategy (SSS). The result shows that, in terms of ADRs with SBC/MRC, the EGT-based APS scheme achieves more than 5% improvement in quality of service (QoS) compared with the SSS-based APS scheme. With the sub-optimum weights of maximum ratio combining (MRC) for ADRs, the EGT-MRC scheme can achieve more than 20 Mbps data rate improvement compared with LiFi systems using single photodiode (PD) receiver.**

***Index Terms*—LiFi, access point selection, evolutionary game theory, angle diversity receiver.**

I. Introduction

Due to the increasing demand for wireless data, which is anticipated to reach 49 exabytes by 2021 [1], the radio frequency (RF) spectrum has become a very limited resource. To support the growth in data traffic and next-generation high-speed wireless communication systems, Light-Fidelity (LiFi) has been introduced as a new wireless access technology. The overall licence-free bandwidth of visible light is more than $1,000$ times greater than the entire RF spectrum. LiFi can provide enhanced security as light does not penetrate through opaque objects [2]. A typical LiFi system uses off-the-shelf low-cost light emitting diodes (LEDs) and photodiodes (PDs) as front end devices [3]. In many large indoor environments, multiple light fixtures are installed, and these luminaries can act as VLC access points (APs). A network consisting of multiple VLC APs is referred to as a LiFi attocell network [4]. LiFi can provide bidirectional and high-speed data communication and enhance physical layer security [5]. These features of LiFi have made it a topic of increased recent research.

In comparison with RF femtocell networks, LiFi attocell networks use smaller cell sizes as the light beams from LEDs are intrinsically narrow [6]. Thus, with the densely deployed optical APs, LiFi attocell networks can achieve a better bandwidth reuse and a higher area spectral efficiency. However, similar to other cellular systems, co-channel interference (CCI) in LiFi attocell networks limits the system performance. This is because in current systems the signal transmitted to a user will interfere with other users who are receiving signals encoded in the same optical spectrum resource. In this case, cell-edge users in particular suffer from severe CCI. Despite the dense deployment of APs, due to CCI, LiFi may not provide uniform coverage with respect to data rate.

An angle diversity receiver (ADR) consists of multiple narrow field of view (FOV) PDs facing in different directions. In [7]–[9], the ADR is used to address the CCI issue as well as the signal to interference plus noise ratio (SINR) fluctuation in LiFi systems, and various signal combining schemes are studied. The AP selection (APS) is important as it determines the combining weights of different combing schemes. However, in these studies, the AP selections are all based on the signal strength strategy (SSS) and only the SINR metric is investigated. In a conventional single PD receiver system suffering CCI, if a user equipment (UE) is allocated to an AP other than the AP providing the best received signal strength, then the AP providing the best signal strength will become the interfering AP. This will cause the signal power to be less than the interference power and the SINR to be less than 0 dB. In other words, only the AP with the best signal strength can provide data to the UE. Hence, the sensible and practical APS in LiFi systems with a single PD receiver is the SSS scheme. However, the situation is different for a LiFi system with ADRs as ADRs can greatly reduce CCI. APS has been studied for LiFi/WiFi hybrid networks in [10], [11]. In [10], the evolutionary game theory (EGT) based load balancing (LB) scheme is adopted, however, the APS scheme in the stand-alone LiFi system is still SSS. The EGT-based LB is only used to select between the best LiFi and WiFi APs.

In this study, we will propose an EGT-based APS scheme considering handover for the stand-alone LiFi system using ADRs. In the EGT-based APS, each user takes individual decisions on the APS by maximising their own quality of service (QoS) and the APS strategy will be adapted iteratively until no user can achieve a better QoS in the network. The SSS-based APS scheme and the single PD receiver will be used as the benchmark. QoS and average user data rate are the performance metrics. The rest of the paper is organised as follows. The LiFi system model is presented in Section II. The EGT-based APS scheme is introduced in Section III. The results are discussed in Section IV and the conclusions are given in Section V.

II. LiFi System model

A. LiFi Channel Gain

In this study, an indoor LiFi network is considered, where N_l LiFi APs are deployed. The set of LiFi APs is denoted by $\mathcal{A} = \{a \mid a \in [1, N_l]\}$. The set of users is denoted as $\mathcal{U} = \{\mu \mid \mu \in [1, N_{\mathrm{UE}}]\}$. The set of users allocated to the AP a is denoted as $\mathcal{U}_a$ and the number of users served by this AP is M_a. Each LiFi AP is composed of several low power LEDs for signal emission, and the total optical power of each LiFi AP is denoted by P_{tx}. In terms of the receiving device, instead of a single PD receiver, an angle diversity receiver with multiple PDs is used. The set of PDs on an ADR is denoted as $\mathcal{P} = \{p \mid p \in [1, N_{\mathrm{PD}}]\}$. According to [12], the LiFi channel impulse response between a-th AP and p-th PD for user μ in the frequency domain is given by:

$$H_{a,\mu,p}(f) = H_{\mathrm{LOS}} H_{\mathrm{F}}(f), \tag{1}$$

where H_{LOS} is the path loss of the line-of-sight (LOS) channel and $H_{\mathrm{F}}(f)$ is the front-end device frequency response. The LOS channel fading gain between the transmitter (Tx) and receiver (Rx) can be modelled as follows [13]:

$$H_{\mathrm{LOS}} = \frac{(m+1)A_{\mathrm{p}} n_{\mathrm{ref}}^2}{2\pi d^2 \sin^2(\Psi_{\mathrm{c}})} T_{\mathrm{s}}(\psi) \cos^m(\phi) \cos(\psi) v_{\mathrm{Rx,Tx}}, \tag{2}$$

where A_{p} is the physical area of the PD; m is the Lambertian order which is given as $m = -\ln(2)/\ln(\cos(\Phi_{1/2}))$ with $\Phi_{1/2}$ denoting the half-power semi-angle of the LED; d represents the distance between the AP and the receiver; n_{ref} denotes the internal refractive index of the concentrator and Ψ_{c} denotes the field of view of the PD; ϕ is the irradiance angle of the transmitter; ψ is the incidence angle of the receiving PD; T_{s} is the gain of the optical filter; $v_{\mathrm{Rx,Tx}}$ is the visibility factor, which is equal to one if the transmitter and receiver are visible to each other, and it is equal to zero if not. In other words, $v_{\mathrm{Rx,Tx}} = 0$ if $\phi > \pi/2$ or $\psi > \Psi_{\mathrm{c}}$.

The distance vector from a user to a LiFi AP is denoted as $\mathbf{d} = (x_{\mathrm{a}} - x_{\mathrm{u}}, y_{\mathrm{a}} - y_{\mathrm{u}}, z_{\mathrm{a}} - z_{\mathrm{u}})$ while the normal vector of the receiving PD is $\mathbf{n}_{\mathrm{PD}}$. The angle of incidence to the PDs can be written as $\psi = \arccos < \mathbf{n}_{\mathrm{PD}}, \mathbf{d} >$, where $<,>$ is the inner product operator. The front-end device frequency response is given in [14]:

$$H_{\mathrm{F}}(f) = \exp - \left(\frac{f}{v_e f_0} \right), \tag{3}$$

where f_0 is the cut-off frequency of the front-end filtering effect; $v_e = 2.88$ is the fitting coefficient which achieves $|H_{\mathrm{F}}(f_0)|^2 = -3$ dB.

B. Angle Diversity Receiver

In this study, we consider the truncated pyramid receiver (TPR) proposed in [9] which is especially suitable for hand-held devices. The TPR is composed of a ring of $N_{\mathrm{PD}} - 1$ inclined side PDs equally separated around the N_{PD}-th central PD. The side PDs are arranged uniformly in a circle on the horizontal plane. In terms of the normal vector of each PD, it is characterized by two angles: the azimuth angle of a PD, ω_{PD}, and the elevation angle of a PD, θ_{PD}, which is the angle between the normal vector of the PD, $\mathbf{n}_{\mathrm{PD}}$, and the UE, $\mathbf{n}_{\mathrm{UE}}$. In terms of the $N_{\mathrm{PD}}-1$ side PDs on a TPR, they have identical elevation angles denoted as Θ_{PD}. Hence, the elevation angles can be expressed as:

$$\theta_{\mathrm{PD}}^p = \begin{cases} \Theta_{\mathrm{PD}}, & 1 \le p \le N_{\mathrm{PD}} - 1. \\ 0, & p = N_{\mathrm{PD}}. \end{cases} \tag{4}$$

The azimuth angle ω_{PD} of the p-th PD is denoted as [9]:

$$\omega_{\mathrm{PD}}^p = \begin{cases} \frac{2(p-1)\pi}{N_{\mathrm{PD}}}, & 1 \le p \le N_{\mathrm{PD}} - 1. \\ 0, & p = N_{\mathrm{PD}}. \end{cases} \tag{5}$$

Hence, the normal vector of the p-th PD is obtained as [15]:

$$\mathbf{n}_{\mathrm{PD}}^p = [\sin(\theta_{\mathrm{PD}}^p)\cos(\omega_{\mathrm{PD}}^p), \sin(\theta_{\mathrm{PD}}^p)\sin(\omega_{\mathrm{PD}}^p), \cos(\theta_{\mathrm{PD}}^p)]^{\mathrm{T}}. \tag{6}$$

C. Signal Combining Scheme

LiFi uses intensity modulation (IM) at the transmitter and the direct detection (DD) at the receiver. Therefore, the transmit signals must be positive and real. According to [16], direct current biased optical orthogonal frequency division multiplexing (DCO-OFDM) is used in this study. There are different signal combining schemes such as equal gain combining (EGC), select best combining (SBC) and maximum ratio combining (MRC). An important metric to evaluate the link quality and capacity is the SINR. According to [7], after signal combining, the SINR between user μ and the serving AP a_{s} is given by:

$$\begin{aligned} \gamma_{\mu,a_{\mathrm{s}}}(f) &= \frac{\left(\sum_{p=1}^{N_{\mathrm{PD}}} \tau P_{\mathrm{tx}} w_p H_{a_{\mathrm{s}},\mu,p}(f) \right)^2}{\sum_{p=1}^{N_{\mathrm{PD}}} {w_p}^2 \kappa^2 N_0 B_{\mathrm{L}} + \sum_{a_{\mathrm{i}} \in \mathcal{A} \setminus \{a_{\mathrm{s}}\}} (\tau P_{\mathrm{tx}} \sum_{p=1}^{N_{\mathrm{PD}}} w_p H_{a_{\mathrm{i}},\mu,p}(f))^2} \\ &= \frac{\left(\sum_{p=1}^{N_{\mathrm{PD}}} w_p H_{a_{\mathrm{s}},\mu,p}(f) \right)^2}{\sum_{p=1}^{N_{\mathrm{PD}}} (\frac{w_p \kappa}{\tau P_{\mathrm{tx}}})^2 N_0 B_{\mathrm{L}} + \sum_{a_{\mathrm{i}} \in \mathcal{A} \setminus \{a_{\mathrm{s}}\}} (\sum_{p=1}^{N_{\mathrm{PD}}} w_p H_{a_{\mathrm{i}},\mu,p}(f))^2}, \end{aligned} \tag{7}$$

where τ is the optical to electrical conversion efficiency at the receivers; w_p is the combining weight of PD p; κ is the ratio of DC optical power to the square root of electrical signal power, where $\kappa = 3$ can guarantee only around 0.3% of the signals will be clipped so that the clipping noise can be neglected [17]; N_0 is the noise power spectral density in LiFi link, which is assumed to follow a Gaussian distribution; B_{L} denotes the LiFi baseband modulation bandwidth; according to (1), $H_{a_{\mathrm{s}},\mu,p}(f)$ is the channel gain in the frequency domain between the PD p of user μ and the serving AP a_{s}; $H_{a_{\mathrm{i}},\mu,p}(f)$ is the channel gain in the frequency domain between the PD p of user μ and the interfering LiFi AP a_{i}.

In the EGC scheme, signals from all PDs are combined with equal weights. Hence, $w_p = 1$, for $p \in \mathcal{P}$.

The SBC scheme only selects the information from the PD with the highest received SINR instead of SNR in [7]. Thus, the selected PD is determined by $p_{\mathrm{s}} = \arg\max_{p \in \mathcal{P}} \frac{(H_{a_{\mathrm{s}},\mu,p}(0))^2}{(\frac{\kappa}{\tau P_{\mathrm{tx}}})^2 N_0 B_{\mathrm{L}} + \sum_{a_{\mathrm{i}} \in \mathcal{A} \setminus \{a_{\mathrm{s}}\}} (H_{a_{\mathrm{i}},\mu,p}(0))^2}$ and the weight of each PD is given by:

TABLE I: Modulation and Coding Table

min. SINR or SNR [dB]	Modulation	Code rate	Spectrum efficiency [bits/s/Hz]
-	-	-	0
1	QPSK	0.44	0.8770
3	QPSK	0.59	1.1758
5	16QAM	0.37	1.4766
8	16QAM	0.48	1.9141
9	16QAM	0.60	2.4063
11	64QAM	0.45	2.7305
12	64QAM	0.55	3.3223
14	64QAM	0.65	3.9023
16	64QAM	0.75	4.5234
18	64QAM	0.85	5.1152
20	64QAM	0.93	5.5547

$$w_p = \begin{cases} 1, & p = p_\mathrm{s}. \\ 0, & \text{otherwise}. \end{cases} \tag{8}$$

In MRC, the output signal from each PD is first multiplied by a weight equal to its own SINR before combining. As the SINR for each sub-carrier frequency is different, the weights for each sub-carrier are expressed as:

$$w_p(f) = \frac{(H_{a_\mathrm{s},\mu,p}(f))^2}{(\frac{\kappa}{\tau P_\mathrm{tx}})^2 N_0 B_\mathrm{L} + \sum\limits_{a_\mathrm{i}\in\mathcal{A}\setminus\{a_\mathrm{s}\}} (H_{a_\mathrm{i},\mu,p}(f))^2}, \tag{9}$$

A combining circuit with varying weights for different frequency is complicated to design. For simplicity, the SINR at zero frequency $w_p(0)$ is adopted as the sub-optimum weight for all sub-carriers. In Section IV, we will show that the sub-optimum weight design achieves similar performance to MRC using optimum weights. The weight selection for SBC and MRC are both dependent on the APS scheme which will be discussed in section III-B.

D. Link Data Rate

The number of OFDM sub-carriers used in LiFi is denoted as Q. According to [12], adaptive M-QAM modulation is used on different OFDM sub-carriers due to the frequency selective channel which includes the optical front-end transfer function. Based on the modulation and coding scheme (MCS) given in Table I, the spectrum efficiency achieved on each sub-carrier can be obtained [18]. In LiFi systems, since the baseband bandwidth is B_L, the double-sided OFDM bandwidth would be $2B_\mathrm{L}$. The LiFi link data rate between the user μ and the AP a can be written as [19]:

$$r_{\mu,a} = \frac{2B_\mathrm{L}}{Q} \sum_{i=1}^{\frac{Q}{2}-1} q_\mathrm{L}(i), \tag{10}$$

where $q_\mathrm{L}(i)$ is the spectrum efficiency of the i-th sub-carrier.

E. Resource Allocation

In this study, time division multiple access (TDMA) is used to serve multiple users [10]. The portion of the time resource allocated by the serving AP a to user μ in a single frame is denoted as $k_{\mu,a}$, where $k_{\mu,a} \in [0,1]$ and $\sum_{\mu\in\mathcal{U}_a} k_{\mu,a} \leq 1$. The proportional fairness (PF) scheme is used for the time resource allocation and the system performance is maximised when [10]:

$$k_{\mu,a} = \frac{1}{M_a}. \tag{11}$$

III. Dynamic Load Balancing for LiFi Networks

A. Handover

In a dynamic LiFi system, the central unit (CU) dynamically allocates the APs to users, and each user will be served by a LiFi AP in each quasi-static state. The handover will occur when two different APs serve a user in two neighbouring quasi-static states. During the handover, users will not receive effective data, therefore, the handover overhead causes a certain reduction in the achievable data rate. The handover overhead time, t_H, in an indoor network is in the order of several milliseconds (ms) and it is assumed to be smaller than the time duration of a quasi-static state T_p [20]. As users move randomly in the indoor environment, the APs assigned to users would change according to the user location and orientation. The integer, n, is defined as the sequence number of the state. Assuming that the user μ is served by the LiFi AP $a_\mu^{(n-1)}$ in the state $n-1$, the handover efficiency between the state $n-1$ and state n can be written as:

$$\eta_i = \begin{cases} [1 - \dfrac{t_\mathrm{H}}{T_p}]^+, & i \neq a_\mu^{(n-1)} \\ 1, & i = a_\mu^{(n-1)} \end{cases}, \quad i \in \mathcal{A}, \tag{12}$$

where i is the expected LiFi AP that will serve the user μ in the state n; and the operation $[.]^+$ represents max(.,0).

B. EGT Based APS Scheme

An EGT based load balancing scheme is proposed for the APS and handover. The EGT based scheme is performed at the beginning of each state to determine the serving AP for each user. The evolutionary game for APS in each state can be formulated as follows:

1. Player Set ($\mathcal{U}$)*:* The users in the LiFi network are the players in the game and the set of players is denoted as $\mathcal{U} = \{\mu \mid \mu \in [1, N_\mathrm{UE}]\}$.

2. Strategy Set ($\mathcal{S}_\mu$)*:* In a LiFi network, the strategy set for each player is the set of LiFi APs. Therefore, $\mathcal{S}_\mu = \mathcal{A} = \{a \mid a \in [1, N_l]\}$.

3. Population: In the proposed game, each player should be connected to a LiFi AP. The set of users served by the AP a is $\mathcal{U}_a$ and the population in this set is M_a.

4. Payoff function: The user QoS is considered as the payoff function as it represents the satisfaction level of each user regarding the AP selection. In general, the satisfaction level would increase along with the data rate. However, the user will be fully satisfied when the data rate increases to the required data rate λ_μ and the further increase of data rate will not bring any benefit regarding the QoS. Hence, the payoff function of the user μ served by the AP a is given by:

$$\pi_{\mu,a} = \min\left\{k_{\mu,a}\frac{r_{\mu,a}}{\lambda_\mu}, 1\right\}. \tag{13}$$

In the context of the evolutionary game for APS, the strategy will be adapted iteratively to enhance the payoff. The strategy adaptation process of APS and the corresponding evolution

Algorithm 1 : EGT based centralised AP selection algorithm

1: Initialisation: A random AP from $\mathcal{S}_\mu$ is assigned to player μ; each AP equally allocates the transmission resource to the connected players; the CU calculates the average payoff of each player $\pi_{\mu,a}^{<0>}$ and the average payoff $\bar{\pi}^{<0>}$; and $t \leftarrow 1$. This algorithm is executed by the CU.
2: **for all** players $\mu \in \mathcal{U}$ **do**
3: The CU calculates the mutation probability $p_\mu^{<t>}$ according to (15);
4: The CU generates a random number with uniform distribution between 0 and 1, denoted as δ.
5: **if** $\delta < p_\mu^{<t>}$ **then**
6: The mutation occurs and player μ is assigned to an AP based on (16).
7: **else**
8: Player μ is still assigned to the original AP.
9: **end if**
10: **end for**
11: **for all** APs $a \in \mathcal{A}$ **do**
12: In each cell, the CU equally allocates the transmission resource to all the players based on (11).
13: **end for**
14: $t \leftarrow t + 1$ and repeat from Step 2 until no AP switch occurs.

can be modelled as follows. In the t-th iteration, the global average payoff of all players is denoted as:

$$\bar{\pi}^{<t>} = \frac{1}{N_{\mathrm{UE}}} \sum_{\mu \in \mathcal{U}} \pi_{\mu,a}^{<t>}, \tag{14}$$

where $\pi_{\mu,a}^{<t>}$ is the payoff of user μ in the t-th iteration. The APS strategy of each player in the t-th iteration is based on the player's payoff and the global average payoff in the last iteration, denoted as $\pi_{\mu,a}^{<t-1>}$ and $\bar{\pi}^{<t-1>}$ respectively. The shift of strategy for each player occurs randomly and follows the principle that the player with a lower payoff would be more likely to change its strategy. This is termed as 'mutation and selection mechanism' in EGT [21]. Thus, in the t-th iteration, the mutation probability for a strategy shift is denoted as:

$$p_\mu^{<t>} = \begin{cases} 1 - \dfrac{\pi_{\mu,a}^{<t-1>}}{\bar{\pi}^{<t-1>}}, & \pi_{\mu,a}^{<t-1>} < \bar{\pi}^{<t-1>}. \\ 0, & \pi_{\mu,a}^{<t-1>} \geq \bar{\pi}^{<t-1>}. \end{cases} \tag{15}$$

When a mutation occurs, a new AP is selected in order to maximise the estimated payoff in the current iteration, which is designed as:

$$\begin{aligned} & a_\mu^{<t>} = \arg\max_{i \in \mathcal{S}_\mu} \hat{\pi}_{\mu,a}^{<t>} \\ \text{s.t.} \quad & \hat{\pi}_{\mu,a}^{<t>} = \begin{cases} \eta_i \pi_{\mu,i}^{<t-1>}, & i = a_\mu^{<t-1>}, \\ \eta_i \dot{\pi}_{\mu,i}^{<t>}, & i \neq a_\mu^{<t-1>}, \end{cases} \end{aligned} \tag{16}$$

where $a_\mu^{<t>}$ is the selected AP of the player μ at the t-th iteration; $\dot{\pi}_{\mu,i}^{<t>}$ is the estimated payoff if the player is served by a different AP from $a_\mu^{<t-1>}$ which is denoted as υ for simplicity. When a new user joins the set of users served by AP υ, based on (11), the allocated portion of resources for each user becomes $k_{\mu,\upsilon}^{<t-1>} = \frac{1}{M_\upsilon^{<t-1>}+1}$. Therefore, the estimated payoff of player μ in the t-th iteration is expressed as:

$$\dot{\pi}_{\mu,i}^{<t>} = \min\left\{ \frac{r_{\mu,\upsilon}}{\lambda_\mu (M_\upsilon^{<t-1>} + 1)}, 1 \right\}. \tag{17}$$

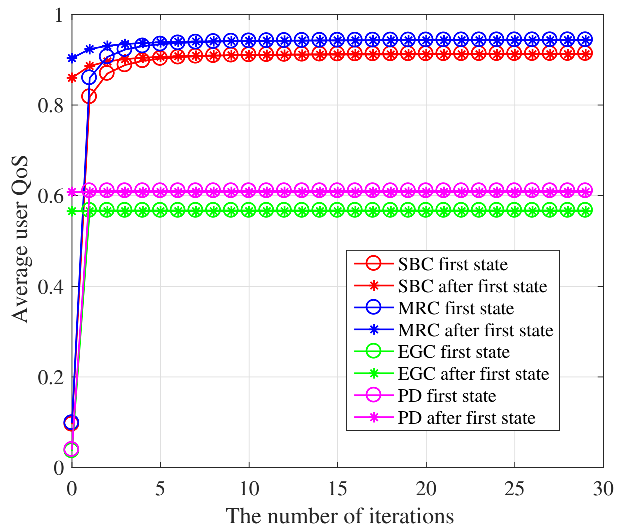

Fig. 1: Convergence analysis of EGT-based APS scheme.

The proposed EGT-based APS algorithm contains the following steps: i) users change their strategies unilaterally to find better serving APs; ii) the transmission resources are equally allocated to the users served by the same AP; iii) repeat step i) and ii) until no user can change the strategy unilaterally to improve their payoff. The EGT-based APS algorithm is summarised in Algorithm 1.

C. Convergence Analysis

In general, an evolutionary equilibrium (EE), referred to as the Nash Equilibrium [10], can be achieved when a convergence is reached.

Definition 1: A strategy profile $\mathcal{E} = \{a_\mu | \mu \in \mathcal{U}\}$ is an EE of the proposed load balancing game if at the equilibrium $\mathcal{E}$, no player can further increase their payoff by unilaterally changing its strategy, i.e.:

$$\pi_{\mu,a_\mu} \geq \pi_{\mu,\beta_\mu}, \quad a_\mu \neq \beta_\mu, \; a_\mu, \beta_\mu \in \mathcal{S}_\mu. \tag{18}$$

To evaluate the required iteration numbers in the proposed APS scheme, computer simulations are used. The simulation parameters are given in Section IV and Table II. The users are considered to be uniformly distributed and they will move randomly for 1000 quasi-static states. At the first state, the initial serving APs are randomly selected. In the following states, the initial serving APs are the selected APs in the last state. As shown in Fig. 1, to achieve an EE, typically around 5 iterations are required for both the SBC and MRC scheme in the first and following states. This means the proposed EGT-based APS scheme achieves fast convergence. For a single PD receiver system, EE will be achieved after the first

TABLE II: Simulation Parameters

Name of Parameters	Value
Height of the UE, z_μ	0.85 m
Optical transmit power in LiFi system, $P_{\rm tx}$	1 W
3 dB frequency of LiFi front-end filtering effect, f_0	30 MHz
LiFi modulation bandwidth, $B_{\rm L}$	300 MHz
Noise power spectral density of LiFi, N_0	10^{-21} $\rm A^2/Hz$
The physical area of the single PD, $A_{\rm p}$	1 $\rm cm^2$
Half-intensity radiation angle, $\Phi_{1/2}$	60°
Half angle of the receiver FOV, $\Psi_{\rm c}$	60°
Gain of optical filter, $T_{\rm s}(\psi)$	1.0
Refractive index, $n_{\rm ref}$	1.5
Optical to electrical conversion efficiency, τ	0.53 A/W
Average optical power to electrical power ratio, κ	3
Time duration of a quasi-static state, $T_{\rm p}$	0.5 s
Handover overhead, $t_{\rm H}$	0.05 s
Average user movement speed, $v_{\rm s}$	1 m/s

iteration. This is trivial and not a realistic scenario. Using the EGT-based APS, each UE will be allocated to the AP with the best received signal strength after the first iteration. Further iterations will not adapt the APS strategy. In other words, in a single PD receiver system, the results of EGT-based APS will be the same as the results obtained from a SSS system. This will be illustrated further in Section IV. In terms of the ADR with EGC scheme, the received signal from each PD is combined with equal weights, therefore, the SINR performance is similar to the system with a single PD receiver. From Fig. 1, it can be seen that the EGC scheme also achieves convergence after the first iteration.

IV. Results and Discussions

As shown in Fig. 2a, a 16 m × 16 m × 3 m indoor office scenario is considered, where 16 LiFi APs are deployed following a square topology. All of the users are moving randomly following the random waypoint model [22]. A TPR with a $N_{\rm PD}$ of 7 and $\Theta_{\rm PD}$ of 30° is considered. The FOV $\Psi_{\rm c}$ of each PD on the TPR is set to be 30°. The performance of the single PD receiver is used as the benchmark. The FOV $\Psi_{\rm c}$ of the single PD receiver is set as 60°. For a fair comparison, the total receiving area of PDs on the ADR should be the same that of the single PD receiver. The other parameters used in the simulation are listed in Table II.

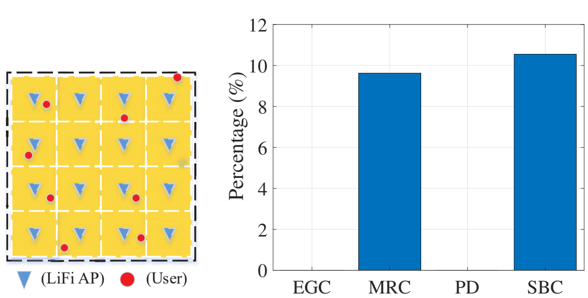

(a) Illustration of the AP deployment.

(b) The percentage of users connecting to other APs other than the AP assigned by the SSS-based APS when EGT-based APS adopted.

Fig. 2

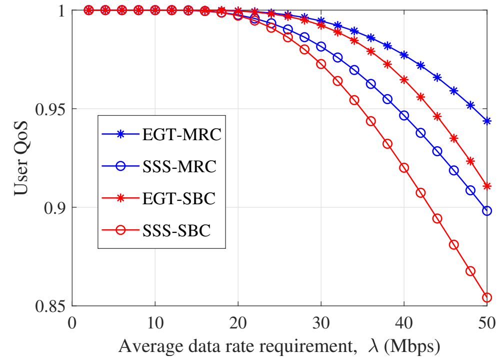

Fig. 3: User QoS versus average required data rate ($N_{\rm UE} = 200$)

When EGT-based APS strategy applied, the percentage of users connecting to other APs other than the AP selected based on the SSS is illustrated in Fig. 2b. In terms of a single PD receiver and ADRs with EGC, 0% means all the UEs are connected to the APs providing the best signal strength. Hence, the AP assignment based on EGT and SSS is the same. This result is expected from the discussion in Section III-C. Due to severe CCI in such systems, excluding the AP with best received signal strength, other APs cannot provide any data to the user. Hence, the SSS scheme is the only sensible and practical APS scheme and the performance of any other scheme will be similar to the SSS scheme. However, as CCI will be greatly mitigated when ADRs with SBC or MRC are considered, around 10% users will choose other APs instead of the AP providing best received signal strength.

The average QoS as a function of the required user data rate is shown in Fig. 3. The number of UEs is assumed to be 200, which is reasonable assuming that there will be many devices in the future. EGT-MRC denotes the EGT-based APS scheme for LiFi systems using ADRs with MRC. Similarly, EGT-SBC, EGT-EGC, SSS-MRC, SSS-SBC, SSS-EGC are defined. EGT-PD and SSS-PD denote the EGT and SSS based APS scheme for LiFi systems using a single PD receiver, respectively. For EGT-MRC, EGT-SBC, EGT-EGC and SSS-MRC, when the average data rate requirement is low, all the users will achieve a QoS of 1. When the average data rate requirement increases to 50 Mbps, it can be seen that the EGT-MRC outperforms the other schemes. The EGT-MRC outperforms the SSS-MRC with QoS of 6%, which is a great improvement. Similarly, compared with the SSS-SBC scheme, the EGT-SBC scheme achieves a 5% increase in QoS. Further increase in the data rate requirement would result in a higher performance improvement of the EGT-based APS scheme compared with the SSS-based APS scheme.

Fig. 4 presents the user QoS of various methods when the average required data rate is 50 Mbps. Three outcomes are observed: i) the QoS of the four methods are equal to 1 for a small number of users, e.g. $N_\mu = 50$; ii) the QoS decreases as the number of users increases, but the QoS of the EGT-MRC scheme decreases much slower than the other methods. When $N_\mu = 200$, users with EGT-MRC and EGT-SBC both achieve a user QoS higher than 0.9, especially for EGT-MRC, the user

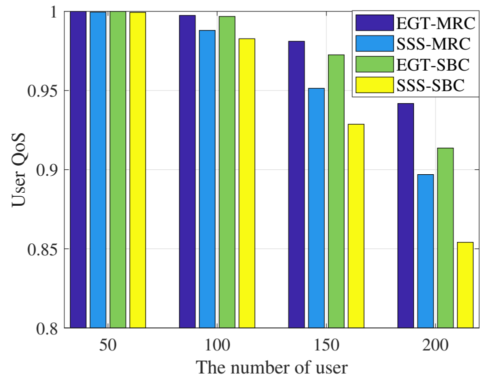

Fig. 4: User QoS versus the number of users ($\lambda = 50$ Mbps)

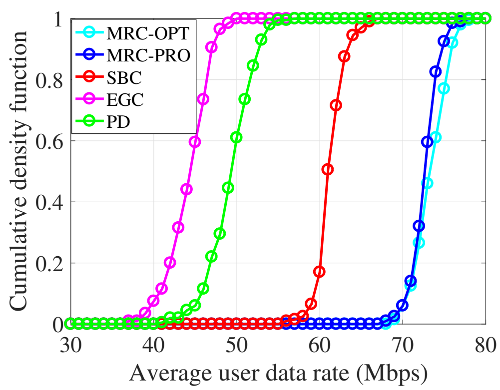

Fig. 5: Cumulative density function of average user data rate for EGT-based APS schemes ($N_{\mathrm{UE}} = 200, \lambda = 50$ Mbps)

QoS is close to 95%, while the SSS based schemes achieve a user QoS below 0.9; iii) with the EGT-based APS scheme, the ADR with SBC outperform the SSS-MRC scheme.

As shown in Fig. 5, the cumulative density function of the average user data rate based on EGT-based APS. It can be seen that the MRC scheme using the proposed sub-optimum weights (MRC-PRO) achieves similar performance to the MRC scheme using the optimum weights (MRC-OPT). Hence, although the weights proposed for MRC-PRO in (9) are not optimum, the sub-optimum weights could achieve similar performance with a much simpler combining circuit. With more than 90% of users achieving a data rate above 70 Mbps, the MRC-PRO scheme outperforms the other three schemes, while around 80% of users achieve a data rate over 60 Mbps for the SBC scheme.

V. Conclusion

In this study, a dynamic LiFi network with angle diversity receivers is considered. An EGT-based AP selection scheme considering handover is proposed. For a single PD receiver system and ADRs with EGC, the proposed scheme has the same performance as the SSS-based APS scheme. However, when the ADR with SBC and MRC are considered, the proposed scheme greatly outperforms the SSS-based APS. The performance gap will increase as the number of users and the required data rate increase. The MRC scheme using the proposed sub-optimum weights achieves similar performance to the MRC scheme using the optimum weights and outperforms all the other schemes.

Acknowledgment

Zeng gratefully acknowledges financial support from pureLiFi Ltd. Soltani acknowledges financial support from the School of Engineering. Wu and Haas acknowledge financial support from EPSRC under grant EP/L020009/1 (TOUCAN).

References

[1] Cisco, "Cisco Visual Networking Index: Global Mobile Data Traffic Forecast Update, 2016–2021 White Paper," *white paper at Cisco.com*, Mar. 2017.

[2] S. Wu, H. Wang, and C. H. Youn, "Visible Light Communications for 5G Wireless Networking Systems: from Fixed to Mobile Communications," *IEEE Network*, vol. 28, no. 6, pp. 41–45, Nov 2014.

[3] D. C. O'Brien, "Visible Light Communications: Challenges and potential." IEEE, October 2011, pp. 365–366.

[4] H. Haas, L. Yin, Y. Wang, and C. Chen, "What is LiFi?" *J. Lightw. Technol.*, vol. 34, no. 6, pp. 1533–1544, March 2016.

[5] M. D. Soltani, X. Wu, M. Safari, and H. Haas, "Bidirectional User Throughput Maximization Based on Feedback Reduction in LiFi Networks," *IEEE Trans. Commun.*, vol. 66, no. 7, pp. 3172–3186, 2018.

[6] T. Borogovac, M. Rahaim, and J. B. Carruthers, "Spotlighting for Visible Light Communications and Illumination," in *2010 IEEE Globecom Workshops*, Dec 2010, pp. 1077–1081.

[7] Z. Chen *et al.*, "Interference mitigation for indoor optical attocell networks using an angle diversity receiver," *J. Lightw. Technol.*, vol. 36, no. 18, pp. 3866–3881, Sept 2018.

[8] Z. Chen, N. Serafimovski, and H. Haas, "Angle Diversity for an Indoor Cellular Visible Light Communication System," in *2014 IEEE 79th Vehicular Technology Conference (VTC Spring)*, May 2014, pp. 1–5.

[9] C. Chen *et al.*, "Reduction of sinr fluctuation in indoor multi-cell vlc systems using optimized angle diversity receiver," *J. Lightw. Technol.*, vol. 36, no. 17, pp. 3603–3610, Sept 2018.

[10] Y. Wang, X. Wu, and H. Haas, "Load Balancing Game With Shadowing Effect for Indoor Hybrid LiFi/RF Networks," *IEEE Trans. Wireless Commun.*, vol. 16, no. 4, pp. 2366–2378, April 2017.

[11] X. Wu, M. Safari, and H. Haas, "Access point selection for hybrid li-fi and wi-fi networks," *IEEE Trans. Commun.*, vol. 65, no. 12, pp. 5375–5385, Dec 2017.

[12] L. Wu, Z. Zhang, J. Dang, and H. Liu, "Adaptive Modulation Schemes for Visible Light Communications," *J. Lightw. Technol.*, vol. 33, no. 1, pp. 117–125, Jan 2015.

[13] J. M. Kahn and J. R. Barry, "Wireless Infrared Communications," *Proceedings of the IEEE*, vol. 85, no. 2, pp. 265–298, 1997.

[14] A. M. Khalid *et al.*, "1-Gb/s Transmission Over a Phosphorescent White LED by Using Rate-Adaptive Discrete Multitone Modulation," *IEEE Photonics Journal*, vol. 4, no. 5, pp. 1465–1473, Oct 2012.

[15] M. D. Soltani, A. A. Purwita, Z. Zeng, H. Haas, and M. Safari, "Modeling the Random Orientation of Mobile Devices: Measurement, Analysis and LiFi Use Case," *IEEE Trans. Commun.*, pp. 1–1, 2018.

[16] C. Chen, D. A. Basnayaka, and H. Haas, "Downlink Performance of Optical Attocell Networks," *J. Lightw. Technol.*, vol. 34, no. 1, pp. 137–156, Jan 2016.

[17] S. Dimitrov and H. Haas, *Principles of LED Light Communications : Towards Networked Li-Fi*, 2015.

[18] H. Burchardt *et al.*, "Distributed and Autonomous Resource and Power Allocation for Wireless Networks," *IEEE Trans. Commun.*, vol. 61, no. 7, pp. 2758–2771, July 2013.

[19] D. Tsonev *et al.*, "A 3-Gb/s Single-LED OFDM-Based Wireless VLC Link Using a Gallium NitrideμLED," *IEEE Photon. Technol. Lett.*, vol. 26, no. 7, pp. 637–640, April 2014.

[20] M. Kassab *et al.*, "Fast and Secure Handover in WLANs: An Evaluation of the Signaling Overhead," in *2008 5th IEEE Consumer Communications and Networking Conference*, Jan 2008, pp. 770–775.

[21] P. Semasinghe, *et al.*, "An Evolutionary Game for Distributed Resource Allocation in Self-Organizing Small Cells," *IEEE Trans. Mobile Comput.*, vol. 14, no. 2, pp. 274–287, Feb 2015.

[22] C. Tsao *et al.*, "Link Duration of the Random Way Point Model in Mobile Ad Hoc Networks," in *IEEE Wireless Communications and Networking Conference (WCNC)*, vol. 1, Apr. 2006, pp. 367–371.